ACS Catalysis

RESEARCH ARTICLE

pubs.acs.org/acscatalysis

Yolk−Shell Catalyst of Single Au Nanoparticle Encapsulated within Hollow Mesoporous Silica Microspheres

Shengnan Wang, Minchao Zhang, and Wangqing Zhang*

Key Laboratory of Functional Polymer Materials of Ministry of Education, Institute of Polymer Chemistry, Nankai University, Tianjin 300071, China

Supporting Information

ABSTRACT: Synthesis and catalysis of yolk−shell microspheres containing a single Au nanoparticle core and a mesoporous shell of hollow mesoporous silica microspheres (HMSM) are reported. This synthesis employs polystyrene-*co*-poly(4-vinylpyridine) microspheres as both template to fabricate the HMSM shell through sol−gel process and scaffold to immobilize the Au nanoparticle. Since the single Au nanoparticle core is supernatant within the inert HMSM shell, the yolk−shell catalyst has minimum support effect and is a promising model to explore the origin of Au catalysis. Catalyzed reduction of 4-nitrophenol with $NaBH_4$ demonstrates size-dependent induction or activation and size-dependent activity of the Au nanoparticle core of the yolk−shell catalyst.

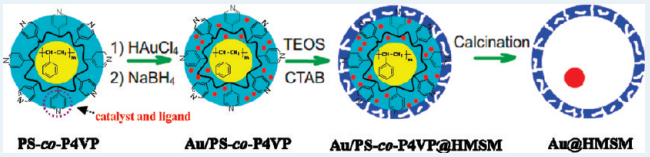

KEYWORDS: Au nanoparticles, catalysis, hollow mesoporous silica microspheres, sol−gel process, yolk−shell catalyst

1. INTRODUCTION

Gold had long been disregarded for catalytic applications due to its inert nature in the bulk state. However, since Haruta et al. discovered a remarkable activity of supported Au nanoparticles in CO oxidation,[1] catalysis by Au nanoparticles has received considerable interest.[2] To date, the catalysis origin of Au nanoparticles has been extensively debated in the literature, and a large number of explanations have been proposed.[3−8] It is deemed that the catalytic activity of Au nanoparticles is ascribed to the nature of surface Au atoms,[9−11] the interaction between the Au nanoparticles and the support,[12−16] or the combination of the two effects.[17] Unfortunately, there is still no clear picture with respect to the origin of Au catalysis, and often, the results reported in the literature concerning Au catalysis are contradictory. To gain further insight into this controversial issue, a suitable model Au catalyst, in which the support effect is isolated from other factors, should be prepared. Generally, a colloidal deposition method is deemed to be an alternative.[18,19] Following this method, Au nanoparticles are generated before they are deposited onto the support, and therefore, influence of the support is weakened or eliminated, whereas agglomeration of Au nanoparticles may occur during the deposition. This makes the synthesis of a qualified Au model catalyst a challenge.

Recently, yolk−shell or rattle-type microspheres have received considerable attention.[20−22] Yolk−shell microspheres possess a unique structure of a hollow shell and an encapsulated, single-nanoparticle core. Yolk−shell microspheres are different from core−shell ones, in which there exists interstitial space between the shell and the nanoparticle core and, therefore, the nanoparticle core is freely movable within the hollow shell. Various methods have been proposed to fabricate yolk−shell microspheres, and most approaches rely on template-assisted synthesis.[20−23] Recently, a yolk−shell catalyst containing a single noble metal nanoparticle core has been studied, and its superiority of stability at high temperature has been demonstrated.[24,25] Since the metal nanoparticle core is supernatant but not deposited on the support, a yolk−shell catalyst is expected to have minimum support effect if an inert hollow shell is employed.

Herein, a general strategy for synthesis of yolk−shell microspheres of a single Au nanoparticle core encapsulated within the inert shell of hollow mesoporous silica microspheres (HMSM) is reported, and the catalysis of the resultant Au@HMSM yolk−shell microspheres is checked. The mesoporous shell of HMSM is employed, since Au nanoparticles supported on the inert silica exhibit lower catalytic activity for various reactions than those on the reducible oxides, such as TiO_2 and CeO_2,[26−28] and therefore, the support effect can be minimized. Furthermore, the mesoporous shell of HMSM presents no substantial mass transfer resistance for reactants.[29] Thus, the Au@HMSM yolk−shell catalyst is expected to be the suitable one to explore the origin of Au catalysis. Model reaction of reduction of 4-nitrophenol with $NaBH_4$ demonstrates an interesting size-dependent induction or activation and size-dependent activity of the Au nanoparticle core of the Au@HMSM yolk−shell catalyst.

Received: November 4, 2010
Revised: December 28, 2010
Published: February 09, 2011

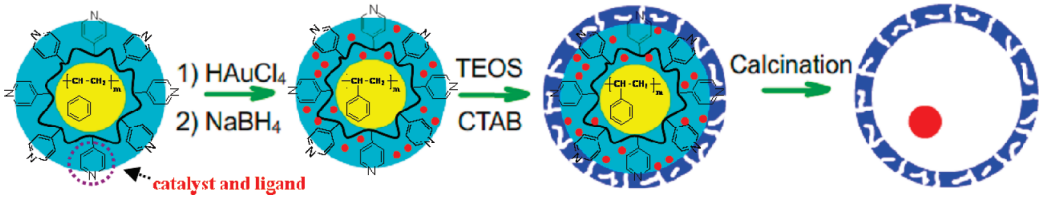

Figure 1. Schematic synthesis of the Au@HMSM yolk−shell catalyst.

2. EXPERIMENTAL SECTION

2.1. Materials. The polystyrene-*co*-poly(4-vinylpyridine) (PS-*co*-P4VP) core−shell microspheres, which were synthesized by one-stage, soap-free emulsion polymerization as discussed elsewhere,[30] were dispersed in water; the polymer concentration was 0.080 g/mL. Tetraethyl orthosilicate (TEOS, >99%, Alfa Aesar), cetyltrimethylammonium bromide (CTAB, >99%, Tianjin Chemical Company), $HAuCl_4 \cdot 3H_2O$ (>99.9%, Tianjin Chemical Company), $NaBH_4$ (>98.9%, Tianjin Chemical Company), $K_2S_2O_8$ (>99.5%, Tianjin Chemical Company), and 4-nitrophenol (>99.5%, Tianjin Chemical Company) were analytical reagents and were used as received.

2.2. Immobilization of Dispersed Au Nanoparticles on PS-*co*-P4VP Core−Shell Microspheres. To immobilize dispersed Au nanoparticles on the PS-*co*-P4VP core−shell microspheres, a given amount of 9.7 mmol/L $HAuCl_4$ aqueous solution was added into 10.0 mL of aqueous dispersion of the PS-*co*-P4VP microspheres, where the molar ratio of 4-vinylpyridine (4VP) to $HAuCl_4$ was 16/1, 32/1, 64/1, and 128/1. The mixture was initially kept at room temperature for 10 h with magnetic stirring, and then the pH value was adjusted to ∼7 with NaOH aqueous solution. Subsequently, a 10-fold excess volume of 20.0 mmol/L $NaBH_4$ aqueous solution was added dropwise with vigorous stirring. The resultant Au nanoparticles immobilized on the PS-*co*-P4VP microspheres of Au/PS-*co*-P4VP were purified by centrifugation, washed thrice with water, and then dispersed in 10.0 mL of water for next use.

2.3. Synthesis of the Au@HMSM Yolk−Shell Microspheres and HMSM Microspheres. TEOS (6.64 g, 31.9 mmol) was added into 90.0 mL of water containing CTAB in which the molar ratio of TEOS/CTAB was set at 2/1. The mixture was initially dispersed by means of an ultrasonic bath set at 20 °C for about 30 min (KQ-200KDE, 40 kHz, 200 W, Zhoushan, China), and then 10.0 mL of the dispersion of the Au/PS-*co*-P4VP microspheres was added. The sol−gel process of TEOS was performed at room temperature for 40 h with vigorous stirring. The resultant silica-coated Au/PS-*co*-P4VP microspheres of Au/PS-*co*-P4VP@HMSM were collected by centrifugation, washed thrice with water (3 × 10 mL), and dried under vacuum at 50 °C for 12 h. After calcination at 550 °C for 4 h, the Au@HMSM yolk−shell microspheres were obtained. The HMSM microspheres were synthesized in a manner similar to the Au@HMSM yolk−shell microspheres, except that 10.0 mL of the aqueous dispersion of the PS-*co*-P4VP microspheres was employed.

2.4. General Procedures for Catalytic Reduction of 4-Nitrophenol. The catalytic reduction was conducted in a standard quartz cell with a path length of 1 cm at 300 K. Typically, the Au@HMSM yolk−shell catalyst (1.0 mL, 0.020 mmol/L Au catalyst) and 4-nitrophenol (1.0 mL, 0.20 mmol/L) were added. Immediately after further addition of $NaBH_4$ (1.0 mL, 20.0 mmol/L), the absorption spectra were recorded by a Cary 50 UV−vis spectrophotometer equipped with a thermostat. The initial molar ratio of Au/4-nitrophenol/$NaBH_4$ was kept at 1/10/1000.

2.5. Characterization. Transmission electron microscopy (TEM) measurement was conducted on a Philips T20ST electron microscope. The powder X-ray diffraction (XRD) measurement was performed on a Rigaku D/max 2500 X-ray diffractometer. The X-ray photoelectron spectroscopy (XPS) analysis was performed with a Kratos Axis Ultra DLD spectrometer employing a monochromated Al Kα X-ray source (1486.6 eV). The nitrogen adsorption−desorption analysis was carried out at 77 K on a Micromeritics TriStar 3000 apparatus. The analytical data were processed by the Brunauer−Emmett−Teller (BET) equation for surface areas and by the Barret−Joyner−Halenda model for pore size distribution.

3. RESULTS AND DISCUSSION

3.1. Synthesis and Characterization of the Au@HMSM Yolk−Shell Catalyst. The synthesis of the Au@HMSM yolk−shell catalyst is schematically shown in Figure 1. First, dispersed Au nanoparticles are immobilized on the PS-*co*-P4VP core−shell microspheres initially through coordination between the metal precursor of $HAuCl_4$ and the coordinative P4VP shell and followed by reduction with $NaBH_4$ aqueous solution.[30] Subsequently, the mesoporous silica shell is coated on the Au/PS-*co*-P4VP microspheres through a surface sol−gel process of TEOS in the presence of CTAB in a neutral aqueous solution without additional catalyst, since the P4VP segment itself is a catalyst for the sol−gel process.[31,32] Last, the resultant Au/PS-*co*-P4VP@HMSM microspheres are calcined, the polymeric template is removed, and dispersed Au nanoparticles are polymerized into a single one, thereby fabricating the Au@HMSM yolk−shell catalyst. In the synthesis, the PS-*co*-P4VP microspheres have three roles: (1) as a scaffold for immobilization of dispersed Au nanoparticles due to the coordinative P4VP segment,[30] (2) as a template for synthesis of the HMSM shell, and (3) as the pendent P4VP segment as the catalyst for sol−gel process of TEOS.[31,32]

The synthesis of the Au@HMSM yolk−shell microspheres is tracked by TEM. Figure 2A, B shows the TEM images of the template of PS-*co*-P4VP microspheres, the average size of which is 325 nm, and the Au/PS-*co*-P4VP microspheres in which the molar ratio of Au/4VP is 1/16, respectively. Immobilization of Au nanoparticles (∼2 nm) on the PS-*co*-P4VP microspheres is clearly indicated by the dispersed black dots on the microspheres. After the surface sol−gel process of TEOS on the template of the Au/PS-*co*-P4VP microspheres, a thin shell of 26 nm mesoporous silica is coated; therefore, Au/PS-*co*-P4VP@HMSM microspheres are produced, which is confirmed by the slight increase in their size from 325 to 375 nm, as shown in Figure 2C and the mesoporous periphery of the microspheres as shown in Figure 2D.

Herein, it should be pointed out that dispersed Au nanoparticles are not observed in Figures 2C and 2D, which is ascribed in part to their small size and in part to the coated silica shell. After calcination at 550 °C, the polymeric template and CTAB are

dx.doi.org/10.1021/cs1000762 |*ACS Catal.* 2011, 1, 207–211

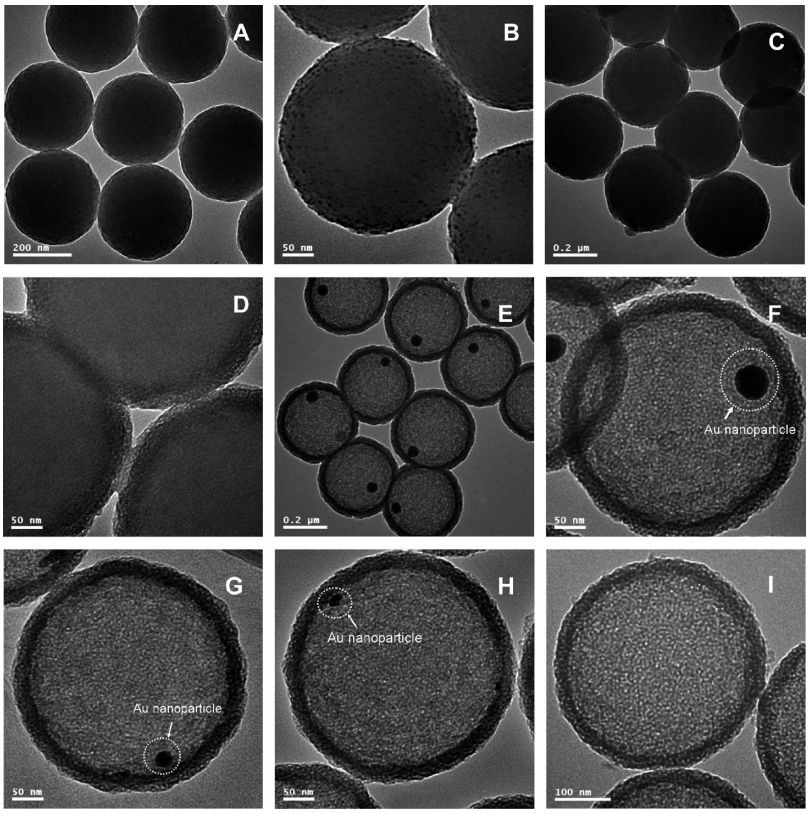

Figure 2. TEM images of the PS-*co*-P4VP microspheres (A), Au/PS-*co*-P4VP microspheres (B), Au/PS-*co*-P4VP@HMSM microspheres (C and D), Au@HMSM yolk−shell microspheres with the size of the Au nanoparticle core at 50 (E and F), 29, (G) and 21 nm (H) and the HMSM microspheres (I).

removed, and the dispersed Au nanoparticles are polymerized into a single Au nanoparticle core of 50 nm; therefore, Au @HMSM yolk−shell microspheres (Figure 2E) are produced.

The polymerization of the dispersed Au nanoparticles into a single nanoparticle core encapsulated within HMSM shell is also confirmed by XRD (Figure S1), UV−vis (Figure S2), and XPS (Figure S3) analysis. Furthermore, from the high magnification TEM image (Figure 2F), the mesoporous structure of the HMSM shell is clearly observed. BET analysis (Figure S4) shows the average size of the mesopore and the surface area of the HMSM shell are 2.8 nm and 347 m^2/g. The mesoporous structure is vital to eliminate mass transfer resistance of reactants in and out of the HMSM shell when the Au@HMSM yolk−shell microspheres are employed as model catalyst. Furthermore, the present method has an advantage of convenient size-tuning of the Au nanoparticle core by changing the molar ratio of Au/4VP. For example, when the molar ratio decreases from 1/16 to 1/64 and further to 1/128, the size of the Au nanoparticle core decreases from 50 to 29 nm (Figure 2G) and to 21 nm (Figure 2H). When no Au precursor is added, HMSM microspheres (Figure 2I) are produced.

Herein, only Au@HMSM yolk−shell microspheres containing the Au nanoparticle core with sizes ranging from 50 to 21 nm are synthesized. It is believed that a smaller Au nanoparticle core can be introduced within the HMSM shell by decreasing the molar ratio of Au/4VP, and this yolk−shell catalyst is expected to be one of the promising candidates for selective hydrogenation.[33,34] However, the present study is focused on the synthesis methodology for a yolk−shell catalyst that has the minimum support effect on catalysis. As discussed in the next section, it is found that the synthesized Au@HMSM yolk−shell catalyst including a large-sized encapsulated Au nanoparticle core shows an interesting size-dependent inhibition and, therefore, is useful to explore the Au catalysis origin.

3.2. Catalysis of the Au@HMSM Yolk−Shell Microspheres. The synthesized Au@HMSM yolk−shell microspheres with different sizes of the encapsulated Au nanoparticle core provide convenience to explore the Au catalysis. The catalysis is checked employing the reduction of 4-nitrophenol to 4-aminophenol with $NaBH_4$ aqueous solution at 300 K as a model reaction. This model reaction has been widely employed to evaluate the catalytic activity of noble metal nanoparticles, and some possible mechanisms have also been proposed.[35−39] This reduction can be monitored by UV−vis analysis, since both 4-nitrophenol and 4-aminophenol have a distinct absorbance in the UV−vis range (λ_{max} = 400 and 290 nm, respectively).[25]

Control experiments demonstrate that the reduction is not catalyzed by the HMSM microspheres or by the $NaBH_4$ aqueous solution. Figure S5 shows a typical example of such a reduction catalyzed by the Au@HMSM yolk−shell catalyst containing a 21 nm Au nanoparticle core, from which the time-dependent conversion of 4-nitrophenol is obtained (Figure 3A). Just as in the general Au nanocatalysts,[9−11] the catalytic activity of the Au@HMSM yolk−shell catalyst is size-dependent. That is, the smaller the size of the Au nanoparticle core of the Au@HMSM yolk−shell catalyst, the faster the conversion of 4-nitrophenol (Figure 3A) and the higher the value of turnover frequency (TOF, which is calculated by moles of product per molar Au per hour when the reduction occurs in the initial 10 min; Figure 3B). Interestingly, it is also found that there exists an inhibition period (ξ) in the reduction, and the ξ is dependent on the size of the Au

dx.doi.org/10.1021/cs1000762 |*ACS Catal.* 2011, 1, 207–211

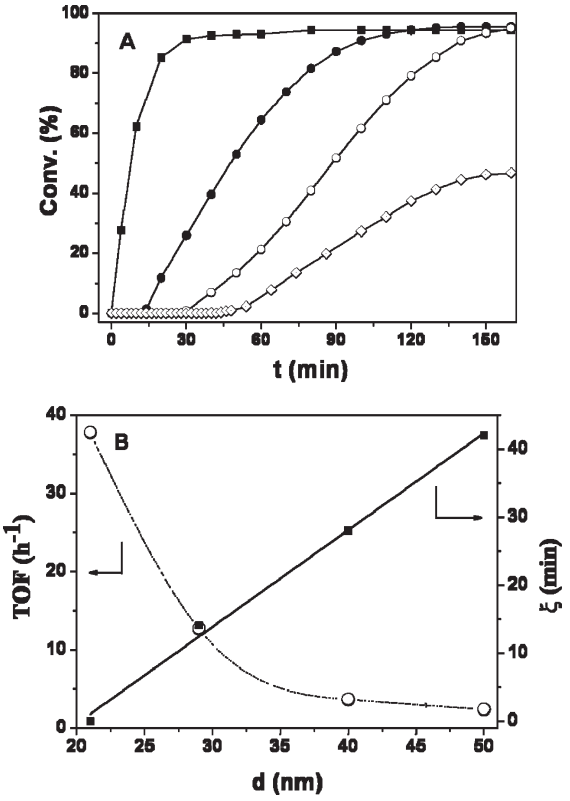

Figure 3. Time-dependent conversion of 4-nitrophenol catalyzed by the Au@HMSM yolk−shell catalyst containing a core of 50 (◊), 40 (○), 29 (●), and 21 nm (■) Au nanoparticles (A), and the size-dependent TOF value (○) and inhibition period ξ (■) of the Au nanoparticle core of the Au@HMSM yolk−shell catalyst (B). Reaction conditions: 6.67 μmol/L Au catalyst, 66.7 μmol/L 4-nitrophenol, 6.67 mmol/L $NaBH_4$, 300 K.

nanoparticle core (Figure 3A). That is, ξ almost linearly increases with the increase in the size of the Au nanoparticle core in the range of 21−50 nm (Figure 3B), and no inhibition is observed when the size of the Au nanoparticle core is smaller than 21 nm.

These results demonstrate that large-sized Au nanoparticle can be activated or inducted for a given time of ξ, and then the catalysis occurs. The exact reason that the Au@HMSM yolk−shell catalyst containing the large-sized Au nanoparticle core has been activated or inducted in the reduction needs further study. Herein, because of the minimum support effect in the Au @HMSM yolk−shell catalyst, both the size-dependent catalysis and the induction or activation of the Au nanoparticle core can be ascribed to the Au nanoparticle core itself.

4. CONCLUSIONS

In summary, synthesis and catalysis of Au@HMSM yolk−shell microspheres containing a size-controlled single Au nanoparticle core and an inert mesoporous shell of HMSM are reported. This synthesis employing PS-*co*-P4VP core−shell microspheres as both template to fabricate mesoporous silica shell through surface sol−gel process and scaffold for immobilization of Au nanoparticles provides convenient size-tuning of the Au nanoparticle core. Because the single Au nanoparticle core is supernatant within the inert shell of HMSM, the Au@HMSM yolk−shell catalyst has minimum support effect and, therefore, is a promising model to explore the origin of Au catalysis. Catalyzed reduction of 4-nitrophenol with $NaBH_4$ demonstrates size-dependent induction or activation and size-dependent activity of the Au nanoparticle core of the Au@HMSM yolk−shell catalyst.

■ ASSOCIATED CONTENT

Supporting Information. Text as well as Figures S1−S5 showing the synthesis and catalysis of the Au@HMSM yolk−shell catalyst tracked by XRD pattern, UV−vis analysis, XPS spectra, and BET analysis. This material is available free of charge via the Internet at http://pubs.acs.org.

■ AUTHOR INFORMATION

Corresponding Author

*Phone: 86-22-23509794. Fax: 86-22-23503510. E-mail: wqzhang@nankai.edu.cn.

■ ACKNOWLEDGMENT

Financial support by the National Science Foundation of China (No. 20974051 & 21074059) and the Tianjin Natural Science Foundation (No. 09JCYBJC02800) is acknowledged.

■ REFERENCES

(1) Haruta, M.; Kobayashi, T.; Sano, H.; Yamada, N. *Chem. Lett.* **1987**, 405.
(2) Corma, A.; Garcia, H. *Chem. Soc. Rev.* **2008**, *37*, 2096.
(3) Su, F.-Z.; Liu, Y.-M.; Wang, L.-C.; Cao, Y.; He, H.-Y.; Fan, K.-N. *Angew. Chem., Int. Ed.* **2008**, *47*, 334.
(4) Mohr, C.; Hofmeister, H.; Radnik, J.; Claus, P. *J. Am. Chem. Soc.* **2003**, *125*, 1905.
(5) Lopez, N.; Janssens, T. V. W.; Clausen, B. S.; Xu, Y.; Mavrikakis, M.; Bligaard, T.; Nørskov, J. K. *J. Catal.* **2004**, *223*, 232.
(6) Chen, M.; Cai, Y.; Yan, Z.; Goodman, D. W. *J. Am. Chem. Soc.* **2006**, *128*, 6341.
(7) Fu, L.; Wu, N. Q.; Yang, J. H.; Qu, F.; Johnson, D. L.; Kung, M. C.; Kung, H. H.; Dravid, V. P. *J. Phys. Chem. B* **2005**, *109*, 3704.
(8) Schwartz, V.; Mullins, D. R.; Yan, W.; Chen, B.; Dai, S.; Overbury, S. H. *J. Phys. Chem. B* **2004**, *108*, 15782.
(9) Panigrahi, S.; Basu, S.; Praharaj, S.; Pande, S.; Jana, S.; Pal, A.; Ghosh, S. K.; Pal, T. *J. Phys. Chem. C* **2007**, *111*, 4596.
(10) Overbury, S. H.; Schwartz, V.; Mullins, D. R.; Yan, W.; Dai, S. *J. Catal.* **2006**, *241*, 56.
(11) Zhou, X.; Xu, W.; Liu, G.; Panda, D.; Chen, P. *J. Am. Chem. Soc.* **2010**, *132*, 138.
(12) Janssens, T. V. W.; Carlsson, A.; Puig-Molina, A.; Clausen, B. S. *J. Catal.* **2006**, *240*, 108.
(13) Sandoval, A.; Gomez-Cortes, A.; Zanella, R.; Diaz, G.; Saniger, J. M. *J. Mol. Catal. A: Chem.* **2007**, *278*, 200.
(14) Haider, P.; Baiker, A. *J. Catal.* **2007**, *248*, 175.
(15) Zhang, X.; Wang, H.; Xu, B.-Q. *J. Phys. Chem. B* **2005**, *109*, 9678.
(16) Milone, C.; Ingoglia, R.; Schipilliti, L.; Crisafulli, C.; Neri, G.; Galvagno, S. *J. Catal.* **2005**, *236*, 80.
(17) Boronat, M.; Concepcion, P.; Corma, A.; Gonzalez, S.; Illas, F.; Serna, P. *J. Am. Chem. Soc.* **2007**, *129*, 16230.
(18) Comotti, M.; Li, W.-C.; Spliethoff, B.; Schuth, F. *J. Am. Chem. Soc.* **2006**, *128*, 917.
(19) Shimizu, K.; Miyamoto, Y.; Kawasaki, T.; Tanji, T.; Tai, Y.; Satsuma, A. *J. Phys. Chem. C* **2009**, *113*, 17803.
(20) Lou, X. W.; Archer, L. A.; Yang, Z. *Adv. Mater.* **2008**, *20*, 3987.
(21) Zhao, W.; Chen, H.; Li, Y.; Li, L.; Li, M.; Shi, J. *Adv. Funct. Mater.* **2008**, *18*, 2780.
(22) Sun, Y.; Wiley, B.; Li, Z.-Y.; Xia, Y. *J. Am. Chem. Soc.* **2004**, *126*, 9399.

(23) Choi, W. S.; Koo, H. Y.; Kim, D.-Y. *Adv. Mater.* **2007**, *19*, 451.
(24) Arnal, P. M.; Comotti, M.; Schuth, F. *Angew. Chem., Int. Ed.* **2006**, *45*, 8224.
(25) Lee, J.; Park, J. C.; Song, H. *Adv. Mater.* **2008**, *20*, 1523.
(26) Arrii, S.; Morfin, F.; Renouprez, A. J.; Rousset, J. L. *J. Am. Chem. Soc.* **2004**, *126*, 1199.
(27) Schubert, M. M.; Hackenberg, S.; van Veen, A. C.; Muhler, M.; Plzak, V.; Behm, R. J. *J. Catal.* **2001**, *197*, 113.
(28) Date, M.; Okumura, M.; Tsubota, S.; Haruta, M. *Angew. Chem., Int. Ed.* **2004**, *43*, 2129.
(29) Djojoputro, H.; Zhou, X. F.; Qiao, S. Z.; Wang, L. Z.; Yu, C. Z.; Lu, G. Q. *J. Am. Chem. Soc.* **2006**, *128*, 6320.
(30) Wen, F.; Zhang, W.; Wei, G.; Wang, Y.; Zhang, J.; Zhang, M.; Shi, L. *Chem. Mater.* **2008**, *20*, 2144.
(31) Khanal, A.; Inoue, Y.; Yada, M.; Nakashima, K. *J. Am. Chem. Soc.* **2007**, *129*, 1534.
(32) Wang, S.; Zhang, M.; Wang, D.; Zhang, W.; Liu, S. *Microporous Mesoporous Mater.* **2011**, *139*, 1.
(33) Claus, P. *Appl. Catal., A* **2005**, *291*, 222.
(34) Bus, E.; Prins, R.; van Bokhoven, J. A. *Catal. Commun.* **2007**, *8*, 1397.
(35) Wunder, S.; Polzer, F.; Lu, Y.; Yu Mei, Y.; Ballauff, M. *J. Phys. Chem. C* **2010**, *114*, 8814.
(36) Wang, Y.; Wei, G.; Zhang, W.; Jiang, X.; Zheng, P.; Shi, L.; Dong, A. *J. Mol. Catal. A: Chem.* **2007**, *266*, 233.
(37) Esumi, K.; Isono, R.; Yoshimura, T. *Langmuir* **2004**, *20*, 237.
(38) Zeng, J.; Zhang, Q.; Chen, J.; Xia, Y. *Nano Lett.* **2010**, *10*, 30.
(39) Zhang, H.; Li, X.; Chen, G. *J. Mater. Chem.* **2009**, *19*, 8223.